Germing surfaces in reaction-diffusion systems? Experiments and a hypothesis

Péter Hantz
Department of Theoretical Physics, Eötvös University, Department of Physical Chemistry, Eötvös University, 1117 Budapest, Pázmány sétány 1/A, Hungary and Department of Plant Taxonomy and Ecology, Eötvös University, 1117 Budapest, Pázmány sétány 1/C, Hungary

(Received 11 March 2002; accepted 16 July 2002)

Simple inorganic reactions in gels, such as $NaOH+CuCl_2$, $NaOH+Cu(NO_3)_2$, and $NaOH+AgNO_3$, are used to obtain complex spatial patterns. When the reactions are running in a thin gel sheet, trapezoid-shaped precipitate regions emerge behind shrinking reaction fronts. Our experimental results suggest that the reaction fronts, which are segments of the borders of the precipitate regions, act as reactive surfaces where an intermediate compound is formed, and the progression of the fronts require a critical concentration of this compound. This phenomenon was modeled by the combination of reaction-diffusion equations and a generalized cellular automata. The most important qualitative features of the patterns have been reproduced by computer simulations. © *2002 American Institute of Physics.* [DOI: 10.1063/1.1505437]

I. INTRODUCTION

Investigation of pattern formation led to the discovery of numerous new phenomena in physics,[1,2] chemistry,[3–5] and biology.[6–8] Several classes of pattern-forming chemical reactions have been examined in the last decades. Chemical waves in liquids and gels and on catalytic surfaces can yield various spatiotemporal patterns.[9–14] Formation of stationary patterns governed by the Turing instability have also been found experimentally.[15–17] Precipitation in the wake of moving diffusion fronts is another much investigated process that can lead to the formation of a great variety of spatial patterns.[18–33] This class of reactions, which will be our concern as well, involves the Liesegang phenomena, where an outer electrolyte with high concentration penetrates into a gel that contains an inner electrolyte. The reaction can result in a set of well-separated precipitation zones.

Recent investigations showed that the $NaOH+CuCl_2$ and $NaOH+Cu(NO_3)_2$ reactions, while running in a Liesegang-type experimental setup, can produce rotating spirals and targetlike patterns that have been observed only in more complex chemical systems.[34] Beside these primary patterns, the $NaOH+CuCl_2$ and the $NaOH+AgNO_3$ reactions can yield microscopic grids consisting of equidistant sheets of colloidal particles, having wavelengths on the order of 10 μm.[35] The basic element of the formation of primary patterns is the emergence of a trapezoid-shaped precipitate region that forms behind a shrinking reaction front, and finally evolves into a trianglelike area. This is strikingly different from the development of Liesegang patterns, where bands of precipitate emerge, usually in the entire area behind a moving front.

A detailed experimental study of the above processes indicated that they cannot be classified into the currently known families of nonlinear chemical reactions.[36] The patterns are produced by simple inorganic reagents unlike in the Belousov-Zhabotinsky type reactions,[37] and the precipitation proceeds in a different way from the case of the Liesegang phenomena. Although the detailed mechanism of the reaction is unknown, the new process of pattern formation and the unusual properties of the border of the precipitate region need the elaboration of a phenomenological model of the above processes. In the first part of the article experimental results are presented that led to the theoretical description. In the next sections, details of the model are discussed. Results of computer simulations that reproduce the most important characteristics of the pattern formation in thin gel sheets are also presented in the third section.

II. THE DYNAMICS OF PATTERN FORMATION IN GEL SHEETS

Experiments in gel sheets were performed in two setups. In the first one, the poly(vinyl)alcohol or agarose gel having a thickness of 0.2–0.3 mm and containing the inner electrolyte $CuCl_2$, $Cu(NO_3)_2$, or $AgNO_3$ was located between a microscope slide and a cover glass. The reaction was started by putting some droplets of NaOH solution at one of the edges of the cover glass [Fig. 1(a)]. In the second setup, the 40-mm-high and 1.6-mm-thick gel sheet was located between two glass plates of 83×102 mm, and the reaction was started by pouring the outer electrolyte on the top [Fig. 1(b)]. Preparation of the experiments are described in the Appendix.

In the usual case, pattern formation in the $NaOH+CuCl_2$ and $NaOH+Cu(NO_3)_2$ reactions evolves in the following way[34] (Fig. 2): As the diffusion front of the NaOH penetrates into the gel, a region is formed where both reagents are present. The diffusion front is followed by a sharp reaction front, where formation of a precipitate takes place. This precipitate looks blue in reflected light and green in transmitted light, and shows no structure when investigated with optical microscopy. Although there can be a large field behind the diffusion front of the NaOH, the reaction is taking place only at the reaction front, which will be referred to as

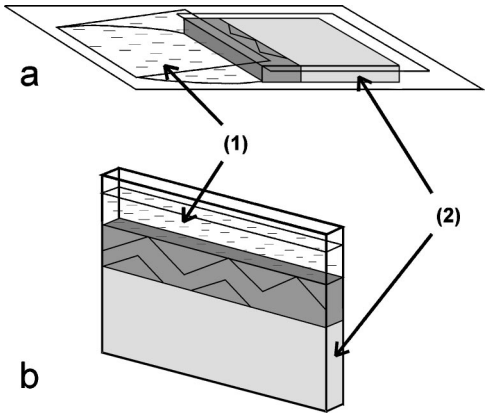

FIG. 1. Experimental setup. The outer electrolyte is denoted by (1), while the inner electrolyte by (2). (a) The gel sheet containing the inner electrolyte is located between a microscope slide and a cover glass. The outer electrolyte is dropped to an edge of the gel sheet, and protected by another cover glass. (b) The gel sheet is located between two glass plates. The outer electrolyte is layered on the gel.

the active border of the precipitate area. Later, in some points of the reaction front the precipitation is halted, and the active border is split into several reaction zones [Fig. 2(a)]. As the front progresses, these points expand into empty regions free of the blue-green precipitate. The precipitation continues on the shrinking reaction zones, which are sweeping through the gel sheet [Fig. 2(b)]. In spite of the presence of both reagents, the reaction does not proceed on the oblique edges that separate the already formed precipitate from the empty regions free of precipitate. These stationary edges will be referred to as passive borders. The reaction continues only on the active borders of the trapezoid-shaped regions. Thus, a reaction zone is a permanently growing and renewing surface.

As the reaction zones sweep through the gel sheet, their length diminishes. Therefore, their margins are referred to as regressing edges [Fig. 2(b)]. At the end of this process, when an active border vanishes, the trapezoid-shaped precipitate region is completed into a trianglelike one, with a small cusp on the top in some cases [Fig. 2(c)]. Due to the similarity of this cusp with some elements of sea shell patterns presented in Ref. 38, the formation will be referred to as the Meinhardt peak.

After a while, when the reagents are recovered by diffusion, new reaction fronts can emerge somewhere along the passive edges, usually at the top of the wedgelike empty regions [Fig. 2(d)]. Later, the new fronts may also be split into reaction zones. Note that formation of new fronts is not included in the phenomenological explanation.

The blue-green precipitate is not the final reaction product. Seven to eight minutes after it has been formed, it starts to convert into a brown colloidal compound. Investigations with x-ray scattering[34] proved that this colloidal compound is CuO. Development of patterns in the $NaOH+AgNO_3$ reaction also goes through the stages described above, except that the primary precipitate formed in the reaction seems to be stable, and does not convert into another compound.

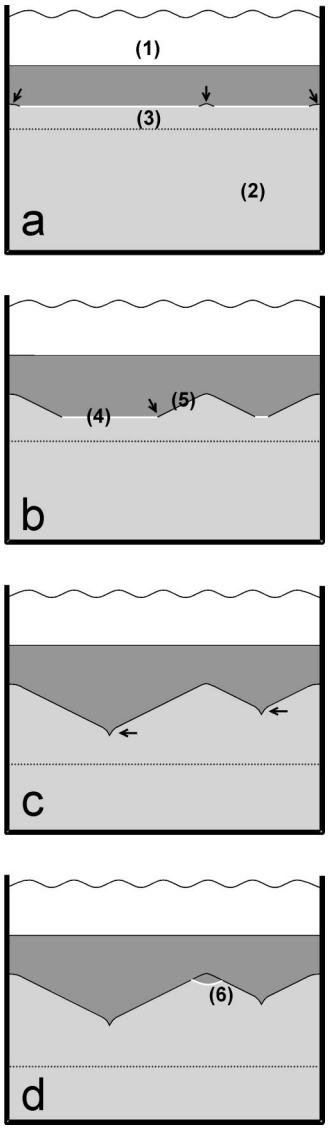

FIG. 2. Schematic diagram on sequence of pattern formation in gel sheets: (1) outer electrolyte, (2) gel sheet containing the inner electrolyte, (3) active region where both reagents are present, (4) shrinking reaction zones, (5) passive borders, (6) new reaction front. The primary precipitate formed in the reaction is drawn in dark gray, while the precipitate-free gel with light gray. The passive borders are marked with black, while the active ones with white curves. Note, that in Ref. 34 the gray color represented the colloidal CuO precipitate, which is not marked here. (a) Progression of the reaction front and that of the diffusion front. The formation of the precipitate is halted in three points of the reaction front, marked by arrows. (b) Shrinking reaction fronts leave behind them trapezoid-shaped precipitate regions. A regressing edge is marked by an arrow. (c) The reaction fronts disappeared, the precipitate triangles are completed. The Meinhardt peaks at the top of the trianglelike regions are marked by arrows. (d) A new reaction front emerged in the top of the wedgelike empty region, where both of the reagents are present.

III. A QUALITATIVE EXPLANATION

The central assumption of the phenomenological explanation is that the sharp reaction zone—the active, growing border of the already formed precipitate—acts as a surface, where the outer and inner electrolytes react, and a diffusive intermediary compound (DC) is formed. Recent ultraviolet–visible microspectrophotometric investigations indicated that in the $NaOH+CuCl_2$ reaction a species different from the

reactants is present in the front of each reaction zone.[39] However, at this time the chemical composition of the DC is unknown.

It is also supposed that the formation of the precipitate and thus the progression of the reaction zone require a critical concentration of the DC. If this concentration is reached on a segment of the active border, a new layer of precipitate will be formed, and in the same time, the DC in the old layer is consumed. Thus, the active edge will be shifted. Otherwise, no new precipitate will form on that section of the active border. Moreover, it is possible that the critical concentration of the DC on a segment of the active border is not reached within a certain time τ, counted from the emergence of the active segment. In this case, the section of the reaction zone looses its reactive property, and becomes part of the stationary, passive border. The reactive surface may act either as a catalyst, or as a germing surface where heterogeneous nucleation and thus formation of the precipitate can take place.[40–42]

The most important qualitative property of pattern formation is the emergence of the trapezoid-shaped precipitate regions in the wake of the reaction zones. In order to understand this feature, the concentration of the DC has to be assumed to be smaller near the end points of the reaction zone than the constant value reached in the middle. Computer simulations showed that this circumstance is typical. If the critical concentration of the DC is smaller than the value in the middle, but larger than the value near the end points of the active border, the next layer of precipitate will be shorter than the reaction zone. For the shrinking to occur, the uncovered portions of the antecedent reaction zone cannot remain reactive too long after the formation of a new layer of precipitate.

Splitting of a reaction front can happen when the front reaches an impurity or inhomogenity present either inside or at the surface of the gel. In such a case, the reaction front is damaged, and therefore may lose its reactive property. As a consequence, the concentration of the DC will be reduced at these points, and passive borders appear as described above.

Development of a small cusp that may appear at the top of the trianglelike precipitate regions cannot be explained by qualitative arguments. This question will be reexamined when the computer simulation results are presented.

Formation of new reaction fronts is attributed to high reagent concentrations. This is the situation at the top of the gel column, when the experiment is started. New fronts can also appear in the top of the wedgelike empty regions. This happens when the reagents consumed by the antecedent reaction zones are recovered by diffusion. Note that emergence of new reaction fronts is not included in the model described in the present article.

The qualitative explanation presented above is supported by several experimental results that were obtained in various setups. The most important observations are enumerated below:

(i) Active and passive borders have different shades of colors in the $NaOH+CuCl_2$ system [Fig. 3(a)]. The passive border has an opalescent shade, unlike the growing, active one. This difference also suggests that the active and passive borders have different structures.

(ii) An interesting phenomenon can occur when a reaction front that is moving along a passive border reaches the top of a precipitate triangle. Figures 3(b) and 3(f) represent the stage when one of the margins of the reaction front moves along a precipitated area. The passive border of a previously formed precipitate is assumed to act as an obstacle where the diffusive intermediary compound cannot penetrate. Therefore, the concentration of the DC is not diminished at this front margin. As the reaction front approaches the top of the precipitated triangle, the DC around this end of the front starts to diffuse in a much larger area then previously. As a consequence, its concentration will diminish. If it drops below the critical concentration required for the progression of the active edge for a time longer than τ, the end point of the reaction front loses its reactive property, and an active–passive transition takes place [Figs. 3(c) and 3(g)]. Later, the portion of the reaction zone that is still active will shrink and evolve as described in the previous paragraphs. The same scenario can take place when a reaction front passes through an obstacle with sharp edges.

(iii) When a segment of a front faces an obstacle such as an air bubble or a splint of glass of about 0.1–1 mm, the speed of that front portion increases before it touches the barrier [Fig. 3(h)]. The speed-up begins when the front is at about 60 μm distance from the obstacle. If the diffusive intermediary compound cannot pass through the barrier, its concentration may increase between the obstacle and the front. The higher concentration of the DC may be the most probable reason for the higher front velocity.

(iv) When two reaction fronts meet and melt together, the front speed is highly increased around the meeting point[35] [Fig. 3(i)]. This speed-up can be explained knowing that in the fronts of both active borders there is a region where the DC is present. At the immediate neighborhood of the meeting point these regions are overlapping and the concentration of the DC is increased. Fronts are supposed to have greater velocity while sweeping through this area. Note that the concavely curved shape of the front also causes an increase in the velocity.

IV. THE MATHEMATICAL MODEL

The mathematical model elaborated for the description of the investigated chemical systems is a combination of partial differential equations[43] and a cellular automata.[44,45] Generalized cellular automata with some of the local variables being continuous was included in order to handle the processes involving the sharp, bandlike reaction front. This problem could also be handled by differential equations having appropiate boundary conditions at the moving fronts, but the cellular automata approach seemed to be more convenient. Note that the reaction-diffusion equations of the model are also discretized in order to perform the simulations. Thus, the whole approach can be regarded as a cellular automata.

This dimensionless model describes the most simple situation: The reaction front propagates in a region where initially both reagents have constant concentration. In a good

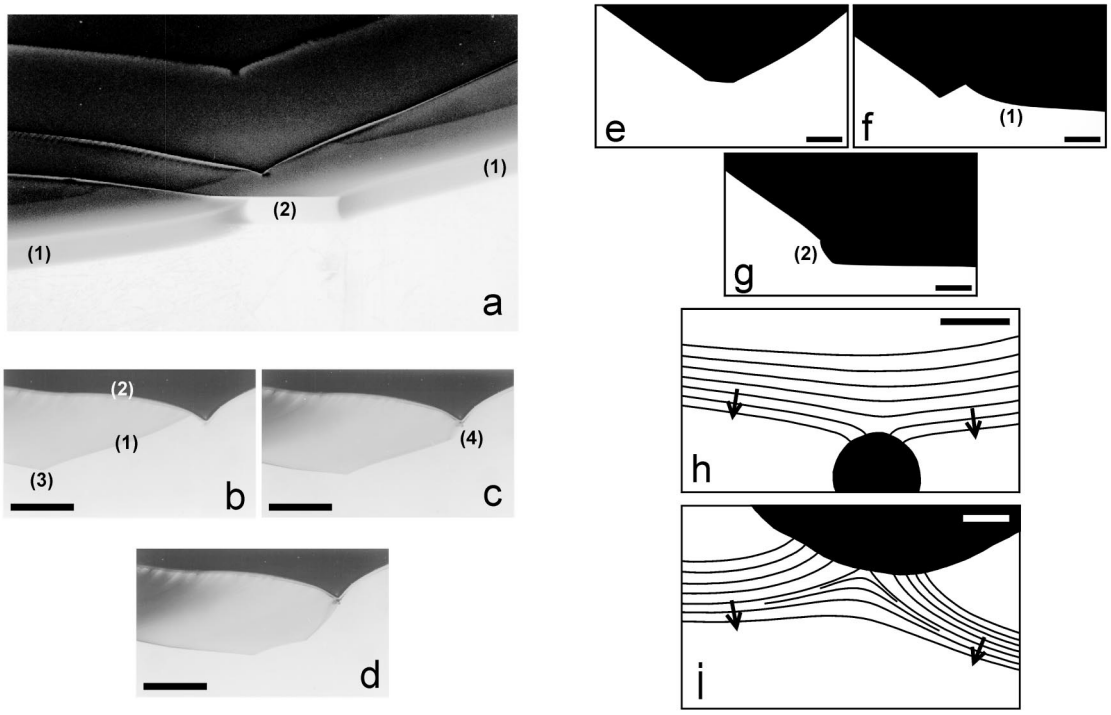

FIG. 3. Experiments supporting the phenomenological model. The outer electrolyte concentration is denoted by a_0, while the inner electrolyte concentration by b_0. (a) Active (1) and passive (2) edges in the NaOH+$CuCl_2$ system in PVA gel, from an oblique point of view. The gel sheet is located between two glass plates. Note their difference with respect to the shade of the colors. $a_0=8M$ NaOH, $b_0=0.732M$ $CuCl_2$, the thickness of the gel sheet is 1.6 mm. (b)–(d) Active–passive transition in the NaOH+$CuCl_2$ system. The reaction is taking place in agarose gel located between two glass plates. $a_0=4M$ NaOH, $b_0=0.586M$ $CuCl_2$, scale bar=2 mm. Time elapsed from the taking of panel (b) is 871 s [panel (c)] and 1398 s [panel (d)], respectively. The reaction zone (1) is bounded on one side by the passive border of a previously formed precipitate (2), and on the other side by a regressing edge (3), which is the meeting point of the reaction zone and a passive border of the novel precipitate [panel (b)]. When the reaction zone reaches the top of the precipitate triangle, a new passive edge (4) will appear [panel (c)]. The reaction zone became bordered by two regressing edges, and thus it will shrink [panel (d)], and later it disappears. Note the decay of the blue-green precipitate into the brown one. (e)–(g) Active–passive transition in the NaOH+$AgNO_3$ system. The reaction is taking place in PVA gel located between a microscope slide and a cover glass. $a_0=8M$ NaOH, $b_0=0.412M$ $AgNO_3$, scale bar=0.5 mm. Time elapsed from the taking of panel (e) is 552 s [panel (f)] and 672 s [panel (g)], respectively. Panel (e) shows a shrinking reaction front, which leaves behind a trapezoid-shaped precipitate region. Panel (f) displays a reaction front (1), which approaches the top of the precipitate triangle formed in the previous scenario. When it reaches the top, an active–passive transition takes place, and a new passive edge (2) will appear [panel (g)]. (h) Speed up of a reaction front segment that faces an obstacle. The reaction is taking place in PVA gel located between a microscope slide and a cover glass. The black lines represent the reaction front every 30 s, and the black region the obstacle itself. The arrows indicate the progressing direction of the reaction front. $a_0=8M$ NaOH, $b_0=0.732M$ $CuCl_2$, and the scale bar $=150$ μm. (i) Fusing of reaction fronts in the NaOH+$CuCl_2$ chemical system. The reaction is taking place in PVA gel located between a microscope slide and a cover glass. The black lines represent the reaction front(s) every 30 s, except the two short curves in the middle. These short curves indicate the position of the fused front 5 and 15 s after the moment when the last unconnected front was plotted. $a_0=8M$ NaOH, $b_0=0.732M$ NaOH, and the scale bar $=150$ μm.

approximation, this is the case when a new front emerges and propagates far behind the diffusion front of the outer electrolyte, e.g., in a wedgelike empty region, after the inner electrolyte has been recovered by diffusion. All compounds have zero-flux boundary conditions. Equations and cellular automata rules of the model are the following:

$$\frac{\partial a(x,y,t)}{\partial t}=D_a(d(x,y,t))\Delta a(x,y,t) - ra(x,y,t)b(x,y,t)\delta(d(x,y,t)-1), \quad (1)$$

$$\frac{\partial b(x,y,t)}{\partial t}=D_b(d(x,y,t))\Delta b(x,y,t) - ra(x,y,t)b(x,y,t)\delta(d(x,y,t)-1), \quad (2)$$

$$\frac{\partial c(x,y,t)}{\partial t}=D_c(d(x,y,t))\Delta c(x,y,t) + ra(x,y,t)b(x,y,t)\delta(d(x,y,t)-1), \quad (3)$$

R1: $[c(x,y,t)>c^*]\wedge[d(x,y,t)=1)]$

$\wedge[d(x_{\mathrm{NN}},y_{\mathrm{NN}},t)=0]$

$\rightarrow[d(x_{\mathrm{NN}},y_{\mathrm{NN}},t+\Delta t)=1]$

$\wedge[d(x,y,t+\Delta t)=0.5]$

$\wedge[c(x,y,t+\Delta t)=0]$,

$$\text{R2: } [c(x,y,t)<c^*]\wedge[d(x,y,t)=1)]\wedge[T(x,y,t)\leqslant\tau]\rightarrow T(x,y,t+\Delta t)=T(x,y,t)+1,$$

$$\text{R3: } [c(x,y,t)<c^*]\wedge[d(x,y,t)=1)]\wedge[T(x,y,t)>\tau]\rightarrow d(x,y,t+\Delta t)=0.5,$$

$$\text{R4: } [d(x,y,t)=1]\wedge[d(x_{\mathrm{NN}},y_{\mathrm{NN}},t)>0\forall(x_{\mathrm{NN}},y_{\mathrm{NN}})]\rightarrow d(x,y,t+\Delta t)=0.5,$$

$$D_{a,b}(d(x,y,t))=\begin{cases}\alpha_{a,b}D_{a,b} & \text{if } d(x,y,t)=0.5\\ D_{a,b} & \text{otherwise,}\end{cases}$$

$$D_c(d(x,y,t))=\begin{cases}0 & \text{if } d(x,y,t)=0.5\\ D_c & \text{otherwise.}\end{cases}$$

Terms $a(x,y,t)$ and $b(x,y,t)$ represent the outer and inner electrolytes, $c(x,y,t)$ the diffusive intermediary compound DC, and c^* its critical concentration, while $d(x,y,t)$ the precipitate formed in the reaction. The term $d(x,y,t)$ is not related to concentration. It can take just a few nonzero values denoting the active edge and the passive form of the precipitate, and the different types of the obstacles, respectively. Thus, $d=1$ at the active edge, $d=0.5$ in the other parts of the precipitate regions including the passive edges, and $d=0$ where no precipitate is present. The obstacles that will be discussed later are represented by other nonzero values of d. $T(x,y,t)$ denotes the age, while τ the maximal lifetime of the cells. Nearest neighbors of the cell at the lattice point (x,y) are denoted by $(x_{\mathrm{NN}},y_{\mathrm{NN}})$. The symbol $\wedge$ denotes the logical AND.

Initial concentrations of reagents are constant values a_0 and b_0, respectively. At the beginning, no DC is present in the system. The model does not describe the emergence of the first active cells; therefore a region where $d(x,y,0)=1$ has to be included in the initial conditions.

The Laplace operator in the diffusion term is denoted by Δ. Diffusion coefficients of the reagents in the regions free of precipitate are D_a and D_b. In the domains filled with the passive precipitate these are reduced by factors $\alpha_a<1$ and $\alpha_b<1$. The diffusion coefficient of the DC, denoted by D_c, is zero where the passive precipitate is present. The precipitate cannot diffuse at all.

According to the model, reaction of the inner and outer electrolytes takes place only at the sharp reaction front, where $d(x,y,t)=1$. This assumption is taken into account by the Kronecker delta function δ in the reaction term. This function is zero anywhere except the active edges, where $d(x,y,t)=1$. The reaction, having rate constant r, is supposed to be proportional to the reagent concentrations.

The meaning of the cellular automata rules are the following: Rule 1 describes the progress of reaction fronts. If the concentration of the DC exceeds the critical threshold c^* at a cell of the reaction front, all the nearest neighbors of the cell that are free of precipitate (i.e., $d=0$) become active. On a square lattice these are the first Neumann-type neighbors. The DC is assumed to be consumed during the activation process, and therefore it is eliminated from a cell that activated its surrounding.

The model assumes that only the surface of the precipitate can act as a reactive region. Therefore, the cell that has activated its surrounding has to become passive. This consequence is also included in rule 1.

Rules 2 and 3 implement the assumption that the concentration of the DC has to reach threshold c^* within time τ measured from the emergence of the active cell; otherwise the element will be passivized. Aging of the cell is described by rule 2, and passivization at the end of its lifetime (if it could not activate its surrounding) is governed by rule 3.

Rule 4 describes the second way of passivization, which is a generalization of the passivization algorithm of rule 1. Cells of the active edge are passivized in any configuration, when they become surrounded by either active or passive cells. In addition, an active cell surrounded by precipitate cells and portions of the obstacle also gets passivized.

Note that in the computational implementation of the model, the differential equations are applied first and the cellular automata rules afterwards. The rules act in the order R1-R2-R3-R4.

The model, which has ten free parameters, describes a complicated chemical system. The most important results, however, can be reached by varying only four parameters (the diffusion coefficients and the critical concentration c^*), while the others are fixed to constant values.

Progression of the reaction front occurs as follows: The reaction, which takes place only at the front [which is represented by a row of active cells where $d(x,y,t)=1$], produces the DC represented by the compound c, while reagents a and b are depleted in the surroundings. Although the DC is allowed to diffuse into the ''precipitate-free'' region where $d=0$, its concentration will rise at the front, while age T of the cells at the front is also increasing. Let us assume that the critical concentration c^* is reached before the age of the cells exceeds the lifetime τ. Usually this happens at the same time in a larger front segment. At this moment, the first neighbors of the active cells (which in this configuration are the next row of cells) becomes active, while the ''mother cells'' gets passivized. At the same time the DC gets depleted in the passivized cells, but while the diffusion rate for the passivized cells is zero, the magnitude of the DC in the passivized cells has no influence on the simulation results.

If the concentration of the DC around the end points of the reaction zone is lower than the constant value in the middle of it, the active cells around the end points will not be able to activate their surrounding when the central segment of the front does. However, these cells continue to produce the DC, but at appropiate parameter values they will not reach the critical concentration c^* in their lifetime τ, and they will be passivized when their age T reaches τ. Thus, the active front segment will be shortened.

In order to increase numerical precision, decreasing the mesh size of the space discretization may appear desirable. However, if physical parameters have to be kept constant, rules 1 and 4 need to be changed. Several rows of active cells have to emerge at the same time, and not only the border

cells can be active. Such extensions of the model have not been investigated. Decreasing the time step does not cause similar problems. Since we cannot solve the model analytically, we carried out computer simulations to investigate its properties.

V. SIMULATION RESULTS

Computer simulations were performed on rectangular and triangular grids. The time evolution of the system was computed by explicit simple time marching. The mesh size was of $\Delta s = 1$, and the time step of $\Delta t = 0.01$. The simulation results did not change when time step was diminished by one order of magnitude.

A. The "chemical needle effect"

First, we will present simulation results of an oversimplified scenario, where reagents a and b, having initially constant concentrations, are allowed to react only on a stationary, straight active segment with a constant length, located in the middle of the grid. This setup does not require the cellular automata rules, and shows in a simple way the features of the distribution of compound c around the active segment. These features are similar to those when c is produced by a moving and also shrinking reaction front.

Depending on the parameters, possible distributions of the compound c can be classified in two important categories. The concentration either decreases monotonically as we approach the end points of the active segment [Fig. 4(a)], or it will have two "bumps" before the end points [Fig. 4(b)]. For the bumps to appear, the diffusion coefficient of c has to be smaller than the diffusion coefficient of each reagent. This condition is not a sufficient, only a necessary requirement.

In both cases, the parameters can be chosen in such a way that the concentration of c at the very end of the segment is smaller than the constant concentration in the middle. This is the case in Fig. 4(a) and also in Fig. 4(b). If we assign the reactive line with a reaction zone, and the compound c with the DC, it is obvious that the critical concentration can be chosen in such manner that shrinking of the reaction zone can occur.

The distribution of the compound c that appeared in time step Δt having a 0.01 time unit length [Fig. 4(c)] can be explained as follows: The influx of the reagents to the reaction zone will be proportional to their concentration gradients, which are found to be maximal around the end points of the segment. As a consequence, formation of the product will be maximal at the endpoints of the reaction zone. This scenario shows a similarity with the needle effect in electrostatics, and thus, it will be referred to as the "chemical needle effect."

An analytical explanation of the overall distribution of c is under investigation. In the studied cases this is is mainly determined by the competition between the influx of the reagents a and b and the spreading of c.

As mentioned above, this simulation does not require the cellular automata rules, and thus refinement of the grid could be simply performed. Similar results were obtained when the time step and also the mesh size were halved, using both finite difference and finite volume schemes. The finite volume scheme was implemented on rectangular and triangular grids.

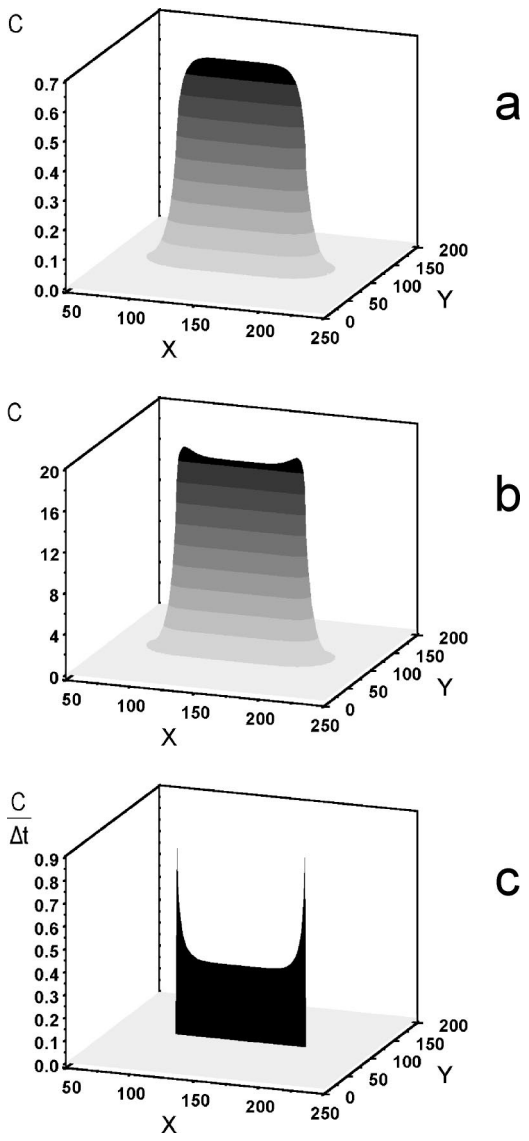

FIG. 4. Computer simulation of concentration profiles of the compound c around a stationary reaction zone. All units are dimensionless. The simulations were performed with the finite difference scheme, on a rectangular grid of 300×200 units. The reaction $a + b \rightarrow c$ is running on a band of unit width and 100 units of length, located in the middle of the grid ($x = 100-199, y = 100$). $t = 5$ time units elapsed from the starting of the reaction. (a) Bumps are not present at the terminations of the reactive segment. $r = 1$, $D_a = 23$, $D_b = 20$, $D_c = 18$, $a_0 = 3$, $b_0 = 1.5$. (b) Bumps were formed near the end points of the reactive segment. Note that before the end points the concentration of c falls below the constant value that was reached in the middle of the segment. $r = 1$, $D_a = 23$, $D_b = 20$, $D_c = 10$, $a_0 = 30$, $b_0 = 15$. (c) Chemical needle effect: The reaction product formed in $\Delta t = 0.01$ is drastically increasing by approaching the end points of the reactive zone. The parameters are the same as in (b).

B. Simulations of pattern-forming processes

These simulations, which reproduced most of the important characteristics of the patterns in gel sheets, have been performed with the finite volume scheme on rectangular grid.

Concentrations and diffusion coefficients were given in the staggered arrangement, which allowed the most effective handling of the space-dependent diffusion.

While $t \leqslant 6$, the active edge where $d(x,y,0)=1$ is located at line $y=50$. This is necessary because the emergence of the first active cells is not included in the model. During this time period, some amount of the DC is also produced, which allows the starting of the front.

After a transient period, the time required for production of the DC necessary for the progression of the active border will not change, and the front reaches a constant speed. As time evolves, this front, which is present on the whole broadness of the diffusion column, moves forward, leaving behind a precipitate region, where $d(x,y,t)=0.5$. Two configurations were studied after the transient period was over. Note that at the moment the detailed chemical mechanism of the reactions is unknown, and thus the parameters of the simulations are not experimentally measured values. However, the diffusion coefficient of the DC is probably smaller than that of the reactants, which has been taken into account in the simulations.

In the first simulation [Figs. 5(a)–5(e)], the passing of the front through two obstacles is studied. In this case, the obstacles are implemented as cells in which the diffusion of all of the diffusive compunds is prohibited. When the front is far from the obstacles, it is planar [Fig. 5(a)], but before touching the barriers, sections of the reaction front close to the them speeds up, in complete agreement with the experiments [Fig. 5(b)].

While approaching the end of the obstacles, the front can behave in two different ways: Either an active–passive transition occurs similar to that described in point (ii) of Sec. III and the front just passed through the gap between the obstacles shrinks, or passivization does not occur, and the front penetrates behind the obstacles.

As mentioned previously, two conditions have to be fulfilled in order to achieve the shrinking of the reaction front. When the critical concentration c^* of the DC in the middle region of the reaction front is just reached, the concentration of the DC around the end points of the front has to be smaller than c^*, and the uncovered portions of the antecedent reaction zone cannot remain active too long after the formation of the new layer of active cells.

After a shrinking-type front passes the barrier, a trapezoid-shaped precipitate area will form behind it, where $d(x,y,t)=0.5$ [Fig. 5(d)]. As the reaction is completed, this evolves into the trianglelike pattern observed in the experiments [Fig. 5(e)].

Meinhardt peaks have been found in the NaOH $+CuCl_2$ reaction system. The model is able to show this pattern, but no set of parameter values has been found where this special termination of the precipitate triangles and the behavior shown in Figs. 5(b)–5(d) are simultaneously present. At the parameter values where the peaks are formed, front propagation terminates before an obstacle due to the depletion of the reagents in the area between the front and the obstacle. When formation of Meinhardt peaks was studied, passivization was induced by two very small obstacles that do not affect diffusion, only prohibit the formation of the DC when they are reached by the reaction front.

A necessary requirement for the Meinhardt peaks to form is the presence of significantly high bumps on the concentration profile of the diffusive intermediary compound. When the reaction front becomes so short that the two bumps of the DC touch each other, the time necessary for the production of the critical concentration of the DC is shortened, and front propagation speed increases. As a result, at the top of the precipitate triangle the Meinhardt peak appears [Fig. 5(f)].

We have to mention that there are several effects that are not described by the present form of the model. In experiments, the excitability of the system, i.e., the ability of raising new fronts and passive edges, grows as the concentration of the inner electrolyte is increased,[34] reagent concentrations are not uniform, and pattern formation takes place at various front speeds. Dependence of the diffusion coefficients on the concentrations[46] are also not included in the model. Note that the parameters of the model are estimates, and not experimentally measured values.

The model does not explain all the qualitative features of the pattern formation, but it has remarkable stability. Parameter regions, where shrinking of the reaction front occurs, are large, e.g., all of the parameters of Figs. 5(a)–5(e) can be varied at least about $\pm 10\%$ without any qualitative change to occur in the patterns.

Several versions of the model, including those where the DC is only a catalyst, led to similar results. Thus, the hypothesis can be considered as a first, rough description of the system, and further experiments are required in order to construct a detailed model of these reactions.

VI. CONCLUSION

The experimental results presented in this article show the most relevant properties of the formation of primary patterns in $NaOH+CuCl_2$, $NaOH+Cu(NO_3)_2$, and $NaOH+AgNO_3$ reactions. Although the detailed mechanism of the reactions is not available at the moment, the phenomenological model discussed above explains the most important characteristics of the pattern formation. These properties, such as shrinking of reaction fronts, formation of Meinhardt peaks, and features of front propagation in the presence of obstacles, have been reproduced by computer simulations. The computational approach outlines some directions for the future experimental research: Characterizing the active borders and finding the diffusive intermediary compound would be of great significance.

ACKNOWLEDGMENTS

I am indebted to Z. Rácz, T. Turányi, L. Hunyadvári, J. Kertész, Gy. Bene, A. Büki, G. Stoyan, and T. Perger for useful discussions; G. Zboray (Eötvös University, Dept. of General Zoology), A. Magyar (Semmelweis University, Dept. of Human Morphology and Developmental Biology), and L. Szilágyi (Eötvös University, Dept. of Biochemistry) for their help in some experiments. I acknowledge the support of E. Szathmáry, E. Keszei, M. Orbán, V. Gáspár, G. Kéri, the Hungarian Research Funds (OTKA T029792), and

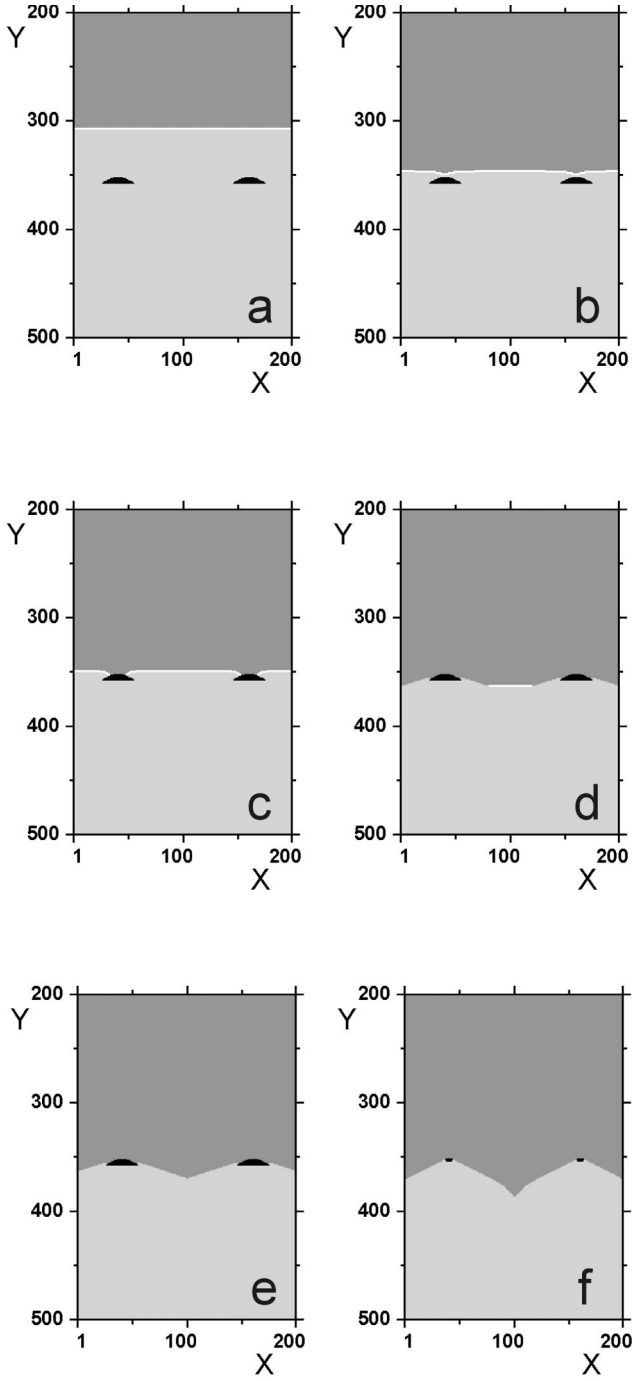

FIG. 5. Simulations of moving reaction fronts. All units are dimensionless. The simulations were performed using the finite volume scheme on a rectangular grid of 200×550 units. The dark gray area represents $d=0.5$, while light gray the regions without any precipitate, i.e., $d=0$. White lines represent the active edges, where $d=1$. The obstacles are drawn in black. (a) The reaction front sweeps through the diffusion column. The obstacles are far, the front is even. The parameters are the following: $r=1$, $c^*=0.66$, $\tau=0.5$, $D_a=23$, $D_b=20$, $D_c=18$, $a_0=3$, $b_0=1.5$, $\alpha_a=0.8$, $\alpha_b=0.5$. Time elapsed from the beginning of the reaction is $t=90$. (b) The reaction front bends towards the obstacles. Time elapsed is $t=103.2$. (c) The front touched the obstacles. Note the similarity with Fig. 3(h). Time elapsed is $t=104$. (d) Regressing edges emerged after the front passed the obstacles. A trapezoid-shaped precipitate region is growing in the central area. Time elapsed is $t=108.9$. (e) The pattern after the termination of the reactions. (f) Precipitate triangle formed at parameter values $r=1$, $c^*=13.3$, $\tau=0.5$, $D_a=23$, $D_b=20$, $D_c=10$, $a_0=30$, $b_0=15$, $\alpha_a=0.8$, $\alpha_b=0.5$. Note the Meinhardt peak in the top of the triangle. The reactions are completed.

the ESF Reactor Program. Additional details are available from the author upon request (hantz@poe.elte.hu or hantz@ludens.elte.hu).

APPENDIX: PREPARATION OF THE EXPERIMENTS

The experiments have been performed either in poly(vinyl)alcohol (PVA), or in agarose gel. The PVA gel was made as follows: 8.6 w/w % PVA solution was prepared by adding PVA powder (PVA 72000, Merck Z.S.) to high-purity water (supplied by Labconco and Millipore filter series) under continuous stirring at 70–80 °C. Complete solubilization was achieved by stirring for 4 h at this temperature, and then it was allowed to cool to room temperature. Inner electrolytes of required concentrations were obtained by adding different amounts of $CuCl_2$ (Merck A.R.), $Cu(NO_3)_2$ (Reanal A.R.), or $AgNO_3$ (Reanal A.R.) solutions to a series of PVA solutions, each of 100.0 ml. Acidity and cross-linking of the gel were set by adding 2.00 ml acid and 1.00 ml of 1.0*M* glutaraldehyde (Merck Z.S.) to the above mixtures. Gels containing inner electrolyte $CuCl_2$ were acidified with 18.50 w/w % HCl (Reanal A.R.), while gels containing $AgNO_3$ or $Cu(NO_3)_2$ with 16.25 w/w % HNO_3, respectively. Then, high-purity water was used to top off each solution to 200.0 ml. After a strong mixing, the air bubbles were driven out by putting the solution into an ultrasonic device for 10–20 s.

To prepare experiments for microscopic investigations, 2–3 droplets of the above solution were placed on a microscope slide, and covered with a cover glass of 22×32 mm. After 1–3 h while the gelation took place, the reactions were started by placing 4–5 droplets of 8.0*M* NaOH outer electrolyte solution (Reanal A.R.) on one of the edges of the gel sheet, and covered with a cover glass to avoid its evaporation.

For the other kind of experiments, the solutions were poured between pairs of glass plates to a height of 50 mm. The 83×102 mm glass plates were placed parallel to each other at a distance of 1.6 mm. In order to fix them, a component of a protein gel electrophoresis device was used. After 10–20 h the reaction was started by pouring 3.00 ml of NaOH outer electrolyte on the top of the gel.

Agarose solution of 2 w/w % was prepared by adding agarose powder (SeaKen, low electroendoosmosis, or Sigma, low EEO) to high-purity water at room temperature. Solubilization was achieved by stirring for 1–2 min at 70–80 °C. In order to obtain inner electrolytes of required concentrations, $CuCl_2$, $AgNO_3$, or $Cu(NO_3)_2$ solutions of 50–60 °C were added to a series of agarose solutions, each of 100 ml. Then, each solution was topped off to 200 ml by high-purity water of 50–60 °C. Cross-linking took place when the above mixtures were allowed to cool down to room temperature. Preparation of the experiments is similar to those with PVA gel, except that experiments can be started in about 1 h, after the temperature of the gel sheets was equalized. All experiments were carried out at room temperature.

Note that in the $NaOH+AgNO_3$ system, when running in a 1.6 mm thick gel sheet, the pattern formation usually stopped after the formation of the first layer of precipitate

triangles; however, when the reaction took place in a thin gel sheet between a microscope slide and a cover glass, a great variety of patterns were formed.

[1] M. C. Cross and P. C. Hohenberg, Rev. Mod. Phys. **65**, 851 (1993).
[2] D. Walgraef, *Spatio-Temporal Pattern Formation* (Springer, New York, 1997).
[3] S. K. Scott, *Oscillations, Waves and Chaos in Chemical Kinetics* (Oxford University Press, Oxford, 1995).
[4] I. R. Epstein and J. A. Pojman, *An Introduction to Nonlinear Chemical Dynamics* (Oxford University Press, New York, 1998).
[5] I. R. Epstein and K. Showalter, J. Phys. Chem. **100**, 13132 (1996).
[6] J. A. Murray, *Mathematical Biology* (Springer, Berlin, 1993).
[7] H. Meinhardt and A. Gierer, BioEssays **22**, 753 (2000).
[8] L. Wolpert, *Principles of Development* (Oxford University Press, Oxford, 1998).
[9] M. Orbán, K. Kurin-Csörgei, A. M. Zhabotinsky and I. R. Epstin, Faraday Discuss. **120**, 11 (2002).
[10] J. Boissonade, E. Dulos, F. Gauffre, M. N. Kuperman, and P. De Kepper, Faraday Discuss. **120**, 353 (2002).
[11] M. Kim, M. Bertram, M. Pollmann, A. von Oertzen, and A. S. Mikhailov, Science **292**, 1357 (2001).
[12] P. Grauel, H. Varela, and K. Krischer, Faraday Discuss. **120**, 165 (2002).
[13] K. Agladze and O. Steinbock, J. Phys. Chem. A **104**, 9816 (2000).
[14] J. I. Hudson and T. T. Tsotsis, Chem. Eng. Sci. **49**, 1493 (1994).
[15] Q. Quyang and H. L. Swinney, Nature (London) **352**, 610 (1991).
[16] K. J. Lee, W. D. McCormick, H. L. Swinney, and Z. Noszticziusz, J. Chem. Phys. **96**, 4048 (1992).
[17] V. K. Vanag and I. R. Epstein, Phys. Rev. Lett. **87**, 228301 (2001).
[18] H. Henish, *Crystals in Gels and Liesegang Rings* (Cambridge University Press, Cambridge, 1988).
[19] T. Antal, M. Droz, J. Magnin, Z. Rácz, and M. Zrínyi, J. Chem. Phys. **109**, 9479 (1998).
[20] S. Kai, S. C. Müller and J. Ross, J. Chem. Phys. **76**, 1392 (1982).
[21] J. George and G. Varghese, Chem. Phys. Lett. **362**, 8 (2002).
[22] I. Lagzi, Phys. Chem. Chem. Phys. **4**, 1268 (2002).
[23] V. Holba and F. Fusek, Collect. Czech. Chem. Commun. **65**, 1438 (2000).
[24] D. A. B. Young, Colloid Polym. Sci. **278**, 464 (2000).
[25] J. H. E. Cartwright, J. M. Garcia-Ruiz, and A. I. Villacampa, Comput. Phys. Commun. **121**, 411 (1999).
[26] M. Chacron and I. L'Heureux, Phys. Lett. A **263**, 70 (1999).
[27] H. J. Krug and H. Brandtstadter, J. Phys. Chem. A **103**, 7811 (1999).
[28] U. Sydow and P. J. Plath, Ber. Bunsenges. Phys. Chem. **102**, 1683 (1998).
[29] N. Curtis and D. G. Leaist, Ber. Bunsenges. Phys. Chem. **102**, 164 (1998).
[30] L. Das, P. Singh, N. R. Agrawal, and R. P. Rastogi, J. Colloid Interface Sci. **192**, 420 (1997).
[31] A. Büki, É. Kárpáti-Smidróczki, and M. Zrínyi, J. Chem. Phys. **103**, 10387 (1995).
[32] T. Antal, M. Droz, J. Magnin, and Z. Rácz, Phys. Rev. Lett. **83**, 2880 (1999).
[33] R. F. Sultan, N. K. Al-Kassem, A. A. H. Sultan, and N. M. Salem, Phys. Chem. Chem. Phys. **2**, 3155 (2000).
[34] P. Hantz, J. Phys. Chem. B **104**, 4266 (2000).
[35] P. Hantz, Phys. Chem. Chem. Phys. **4**, 1262 (2002).
[36] Precipitation patterns with some similar properties have recently been observed in chemical systems where hydrous solutions of copper chloride or other transition metal salts are reacted with potassium ferrocyanide or potassium ferricyanide homogenised in PVA or agarose hydrogels [B. de Lacy Costello *et al.* (unpublished)].
[37] L. Hegedüs, M. Wittmann, Z. Noszticzius, S. Yan, A. Sirimungkala, H.-D. Försterling, and R. J. Field, Faraday Discuss. **120**, 21 (2002).
[38] H. Meinhardt, *The Algorithmic Beauty of Sea Shells* (Springer, Berlin, 1995).
[39] P. Hantz and J. Partridge (unpublished).
[40] R. J. Hunter, *Introduction to Modern Colloid Science* (Oxford University Press, Oxford, 1993).
[41] G. A. Somorjai, *Introduction to Surface Chemistry and Catalysis* (Wiley, New York, 1994).
[42] D. Avnir, *The Fractal Approach to Heterogeneous Chemistry: Surfaces, Colloids, Polymers* (Wiley, Chichester, 1989).
[43] J. H. Ferziger and M. Peric, *Computational Methods for Fluid Dynamics* (Springer, Berlin, 1996).
[44] B. Chopard and M. Droz, *Cellular Automata Modeling of Physical Systems* (Cambridge University Press, Cambridge, 1998).
[45] J. R. Weimar and J.-P. Boon, Phys. Rev. E **49**, 1749 (1994).
[46] T. Erdey-Grúz, *Transport Phenomena in Aqueous Solutions* (Wiley-Akadémiai-Hilger, New York, 1974).